

Identification of TPBG-Expressing Amacrine Cells in DAT-tdTomato Mouse

Wanjing Huang,¹ Qiang Xu,¹ Feng Liu,¹ Jing Su,¹ Dongchang Xiao,¹ Lei Tang,¹ Zhao-Zhe Hao,¹ Ruifeng Liu,¹ Kangjian Xiang,¹ Yalan Bi,² Zhichao Miao,^{2,3} Xialin Liu,¹ Yizhi Liu,^{1,4} and Sheng Liu^{1,5}

¹State Key Laboratory of Ophthalmology, Zhongshan Ophthalmic Center, Sun Yat-sen University, Guangdong Provincial Key Laboratory of Ophthalmology and Visual Science, Guangzhou, China

²European Molecular Biology Laboratory, European Bioinformatics Institute (EMBL-EBI), Wellcome Genome Campus, Cambridge CB10 1SD, United Kingdom

³Translational Research Institute of Brain and Brain-Like Intelligence and Department of Anesthesiology, Shanghai Fourth People's Hospital Affiliated to Tongji University School of Medicine, Shanghai, China

⁴Research Unit of Ocular Development and Regeneration, Chinese Academy of Medical Sciences, Beijing, China

⁵Guangdong Province Key Laboratory of Brain Function and Disease, Guangzhou, China

Correspondence: Sheng Liu, Zhongshan Ophthalmic Center, Sun Yat-sen University, Guangzhou 510060, China;

liush87@mail.sysu.edu.cn.

Yizhi Liu, Zhongshan Ophthalmic Center, Sun Yat-sen University, Guangzhou 510060, China;

yzliu62@yahoo.com.

Xialin Liu, Zhongshan Ophthalmic Center, Sun Yat-sen University, Guangzhou 510060, China;

liuxl28@mail.sysu.edu.cn.

HW, XQ and LF contributed equally to this work.

Received: January 28, 2022

Accepted: April 25, 2022

Published: May 12, 2022

Citation: Huang W, Xu Q, Liu F, et al. Identification of TPBG-expressing amacrine cells in DAT-tdTomato mouse. *Invest Ophthalmol Vis Sci.* 2022;63(5):13. <https://doi.org/10.1167/iovs.63.5.13>

PURPOSE. Neurons are the bricks of the neuronal system and experimental access to certain neuron subtypes will be of great help to decipher neuronal circuits. Here, we identified trophoblast glycoprotein (TPBG)-expressing GABAergic amacrine cells (ACs) that were selectively labeled in DAT-tdTomato transgenic mice.

METHODS. Retina and brain sections were prepared for immunostaining with antibodies against various biomarkers. Patch-sequencing was performed to obtain the transcriptomes of tdTomato-positive cells in DAT-tdTomato mice. Whole-cell recordings were conducted to identify responses to light stimulation.

RESULTS. Tyrosine hydroxylase immunoreactive cells were colocalized with tdTomato-positive cells in substantia nigra pars compacta, but not in the retina. Transcriptomes collected from tdTomato-positive cells in retinas via Patch-sequencing exhibited the expression of marker genes of ACs (*Pax6* and *Slc32a1*) and marker genes of GABAergic neurons (*Gad1*, *Gad2*, and *Slc6a1*). Immunostaining with antibodies against relevant proteins (GAD67, GAD65, and GABA) also confirmed transcriptomic results. Furthermore, tdTomato-positive cells in retinas selectively expressed *Tpbg*, a marker gene for distinct clusters molecularly defined, which was proved with TPBG immunoreactivity in fluorescently labeled cells. Finally, tdTomato-positive cells recorded showed ON-OFF responses to light stimulation.

CONCLUSIONS. Ectopic expression occurs in the retina but not in the substantia nigra pars compacta in the DAT-tdTomato mouse, and fluorescently labeled cells in the retina are TPBG-expressing GABAergic ACs. This type of transgenic mice has been proved as an ideal tool to achieve efficient labeling of a distinct subset of ACs that selectively express *Tpbg*.

Keywords: DAT-Cre, GABAergic amacrine cells, patch-seq, TPBG, TH

Neurons are the unit of complex networks. The mammalian brain contains many millions, and in some cases billions, of neurons. Regularly, we tend to classify them into classes and types based on diverse criteria.¹ Successful access to certain cell subtypes will be of great help for us to further uncover the neuronal circuits. And current applications of optogenetics are commonly accompanied with ever-increasing specificity of direct targeting and modulation.²

Transgenic mouse lines are of great value, not only in constructing disease models,^{3,4} but also in helping us target certain neurons.^{5,6} Sometimes, for several reasons,⁷ transgenic expression occurs at cells where normally endogenous genes do not express,⁸ which may bring unexpectedly profitable outcomes. For example, in the Thy1-lox-

YFP-STOP-lox-wheat germ agglutinin mouse line, the gene wheat germ agglutinin was initially designed to express in retinal ganglion cells (RGCs) labeled by YFP excited by Cre recombinase. However, it turned out that not all RGCs were successfully marked by YFP and that wheat germ agglutinin was undetectable in YFP-positive cells. Instead, a subset of RGCs with the smallest arbors, called W3-RGCs, were marked by YFP,⁹ and therefore have been widely used in several studies.^{10,11} Moreover, in another study,¹² an ectopic mode was revealed in the retina of the ChAT-ChR2-EYFP mouse line. Although EYFP-positive cells were ChAT-positive simultaneously in various brain areas, none of the EYFP cells show detectable ChAT immunoreactivity in the retina. However, non-GABAergic non-glycinergic amacrine

cells (ACs) and a subset of M1 ipRGCs innervating only the suprachiasmatic nucleus were labeled by EYFP.

Dopamine transporter-Cre (DAT-Cre) (B6.SJL-*Slc6a3*^{tm1.1(cre)Bkmn/J}; Strain #006660; Common Name: DAT^{IREScree}) is a well-established transgenic mouse line and has been reported to label dopaminergic neurons in the brain successfully.¹³ Several studies have been conducted to reveal the Cre recombinase expression pattern in some other tissues by crossing DAT-Cre with different tdTom lines, such as Ai9 (Strain #007909), Ai14 (Strain #007914), and Ai34 (Strain #012570).^{8,14–16} However, the gene expression pattern in the retina has not been studied in DAT-tdTomato (Ai9).

There are two types of dopaminergic ACs described in the retina of rhesus monkey,¹⁷ guinea pig¹⁸ and rat,¹⁹ which are all immunoreactive for tyrosine hydroxylase (TH). In rhesus monkey retina, the type 1 cells (in the following referred to as TH1 cells) have large cell bodies located exclusively in the inner nuclear layer (INL), processes in the S1 of the inner plexiform layer (IPL), and much higher levels of TH. The type 2 cells (in the following referred to as TH2 cells) have relatively small cell bodies located in the INL, IPL, and ganglion cell layer (GCL), with processes arborizing in the center of IPL, and contain lower levels of TH.¹⁷ However, there is only one type of AC in the mouse retina that could be stained with TH, and they show characteristics similar to TH1 cells in their primate counterparts.

Retinal dopaminergic neurons have been studied extensively in the mouse.^{20–22} In addition, Zhang et al.²³ reported two types of ACs labeled with transgenic mouse line TH::RFP. One type has a large cell body with processes ramified in S1 of IPL and is TH immunoreactive. The second type has smaller soma, ramifies in S3, and lacks TH.²³ They consider these two types are corresponding with TH1 and TH2 cells in other species. The morphologies and retinal distribution of TH2 cells in the mouse has then been studied. Later, the electrophysiological characteristics of TH2 cell type are extensively studied.^{24,25} Transgenic mouse line TH-Cre Ai9 is reported to selectively label TH2 ACs as well as sparse subsets of dopaminergic ACs and starburst ACs (SACs).²⁶

In this study, we crossed DAT-Cre transgenic mice with Ai9 and found that in the retinas of the offspring, tdTomato-positive cells were TPBG-expressing GABAergic ACs, which stratified in the narrow band between S2 and S3 and showed ON-OFF responses to light stimulation. Considering the multiple cell types labeled by DAT-tdTomato (Ai14),¹⁴ we proved that DAT-tdTomato (Ai9) can serve as a valuable tool for studying the subset of TPBG-expressing GABAergic ACs.

METHODS

Transgenic Mice

Dopamine transporter-Cre (DAT^{IREScree}, Stock No:006660, strain code: B6.SJL-*Slc6a3*^{tm1.1(cre)Bkmn/J}) and Ai9 (Stock No:007909, strain code: B6.Cg-*Gt(ROSA)26Sor*^{tm9(CAG-tdTomato)Hze/J}) mice were obtained from The Jackson Laboratory (Bar Harbor, ME) and bred in Ophthalmic Animal Laboratory, Zhongshan Ophthalmic Center, Sun Yat-sen University. Controlled photoperiods (12 hours light and 12 hours darkness) and sufficient supplies were given in a temperature-controlled room in a specific pathogen-free environment. All procedures were carried out strictly in accordance with the ARVO Statement for the Use of Animals

in Ophthalmic and Vision Research and approved by the Institutional Animal Care and Use Committee of Zhongshan Ophthalmic Center.

Generation and Phenotyping of Mouse Line

DAT-tdTomato were generated by crossing these two mouse lines mentioned elsewhere in this article. Offspring were genotyped for the expression of Cre and tdTomato. For DAT-Cre, the following pair of primers: 5'-TGG CTG TTG GTG TAA AGT GG-3' and 5'-CCA AAA GAC GGC AAT ATG GT-3' were used to detect the presence of Cre recombinase. A 152-bp band should be predicted for mutant Cre mouse. For Ai9/Rosa26-LSL-tdTomato, 5'-AAG GGA GCT GCA GTG GAG TA-3' and 5'-CCG AAA ATC TGT GGG AAG TC-3' were designed as forward and reverse primer respectively for wild type; 5'-CGC ATT AAA GCA TAT CC-3' and 5'-CTG TTC CTG TAC GGC ATG G were designed as forward and reverse primers each for mutant. The predicted band was 196 bp for the mutant tdTomato mouse and 297 bp for the wild-type mouse.

Sample Preparation for Patch-seq

DAT-tdTomato mice that were identified by genotyping were sacrificed and eyeballs were removed. The cornea and lens were removed to isolate the retinas. Retinal slices were made according to the previous research.²⁷ Briefly, a part of the isolated retina was embedded in 2.5% agarose (Sigma-Aldrich, A0701, St. Louis, MO), which was dissolved in the buffer for agarose gel (NaCl 119 mM, HEPES 40 mM, NaH₂PO₄ 1.25 mM, KCl 2.5 mM, CaCl₂·2H₂O 1.15 mM and MgSO₄ 1.5 mM) at 150°C and held at 37°C. This embedded retina was quickly cooled and stuck at the base of the slicer (Leica Biosystems, VT1200s, Wetzlar, Germany). We cut 200-µm-thick slices out and kept them in Ames' medium (Sigma-Aldrich, A1420) saturated with carbogen (95% O₂ and 5% CO₂). Retinal slices were stored in oxygenated Ames' medium at room temperature (RT). For whole-mounted retinas, a piece of retina was cut out and mounted with the ganglion cell side facing up onto a filter paper (Merck Millipore, HAWPO1300, Burlington, MA) with a hole in the center.

Tissue Preparation for Immunohistochemistry

Animals were anesthetized using 0.15 to 0.18 mL sodium pentobarbital (0.01 g/mL sterile water) via intraperitoneal injection followed by transcardial perfusion with normal saline and 4% paraformaldehyde (PFA).²⁸ Eyes were removed and hemisected in 0.01 M PBS (9 g NaCl, 50 mL 0.2 M PB, and 950 mL dH₂O).²⁹ The posterior eye cups were then fixed in 4% PFA for 30 minutes at RT. The eyeballs were cryoprotected at 4°C in 10% (w/v) sucrose solution until the bottom, transferred to the 20% sucrose solution, and then transferred to the 30% sucrose solution overnight. The tissue was embedded in optimal cutting temperature medium and stored at -80°C.^{30,31} The eye cups were sectioned vertically at 15 to 16 µm using CM1850 Cryostat Microtome (Leica Biosystems). The brain tissue was fixed with 4% PFA at 4°C for 6 hours after transcardial perfusion. After that, the brain was washed three times with PBS at the swing bed, 5 minutes each time. Then the brain was transferred to 15% and 30% sucrose solution (w/v in PBS) sequentially. After sinking, the tissue was also embedded in optimal cutting temperature medium and sectioned vertically at 30 µm.

TABLE 1. List of the Primary Antibodies Used in This Study

Antibody	Host	Source	Dilution
GABA	Rabbit	Sigma-Aldrich, A2052	1:1000
5T4	Rabbit	Abcam, ab129058	1:800
TH	Rabbit	Sigma-Aldrich, AB152	1:1000
Calretinin	Rabbit	Abcam, ab92341	1:800
GAD65	Mouse	BD Biosciences, 559931	1:1000
GAD67	Mouse	Millipore, MAB5406	1:1000
GlyT1	Goat	Millipore, AB1770	1:2000
VGluT3	Mouse	Sigma-Aldrich, SAB5200312	1:500
VIP	Rabbit	ThermoFisher Scientific, PA5-78224	1:500
ChAT	Goat	Merck Millipore, AB144P	1:500

Immunohistochemistry

Retinal sections were dried for 30 minutes and then washed with 0.01 M PBS three times for 10 minutes each at RT. Blocking solution consisted of 6% donkey serum in 0.3% Triton X-100 in 0.01 M PBS. The sections were pretreated with the blocking solution for 2 hours at RT and then incubated in primary antibodies diluted in the 3% BSA overnight at 4°C. Retinas were washed with 0.01 M PBS three times for 10 minutes and incubated in secondary antibodies (donkey anti-rabbit Alexa Fluor 488/647-conjugated) diluted in 0.3% Triton X-100 in 0.01 M PBS for 2 hours at RT, washed again and incubated in DAPI for 10 minutes. The retinas were then washed with 0.01 M PBS three times for 10 minutes, mounted with antifade mounting medium (ThermoFisher Scientific, S36972, Waltham, MA) and covered with a coverslip and stored at 4°C until imaging. The staining procedure of brain slices is similar to the retinal slices as previously described.³² Briefly, free-floating brain sections were washed with PBS containing 0.3% Triton-X (PBST) for three times, 5 minutes each time, followed by 1 hour of blocking (10% serum in 0.3% PBST) at RT. The incubation of primary antibodies diluted in 0.3% PBST with 2% serum took place overnight at 4°C. Sections were then washed in 0.3% PBST, incubated with the secondary antibodies and DAPI diluted in 0.3% PBST for 2 hours at RT. Finally, sections were washed in PBST, mounted and coverslipped using the antifade mounting medium. The antibodies used in this study are presented in Table 1.

Image Acquisition and Quantification

The immunostaining images were acquired with Zeiss laser scanning confocal microscopes (Carl Zeiss Meditec, LSM 880; LSM 980, Jena, Germany) and Tissue fax (TissueGnostics, Tissue FAXS Q+, Vienna, Austria). Cells that were tdTomato-positive were targeted to be acquired. Confocal scans were captured using Plan-Apochromat 20 × (N.A. 0.8) dry, 40 × (N.A. 1.2), and 63 × (N.A. 1.4) oil-immersion objective, respectively. A total of 10 to 13 μm thickness with z-intervals between 0.3 and 0.6 μm (1024 × 1024 pixels) were obtained and orthogonal projections were conducted. The number of tdTomato-positive cells and colocalized staining cells were calculated manually using the cell counter function in ImageJ (<https://imagej.nih.gov/ij/>).

Recording Light-evoked Responses

Mice were maintained in darkness overnight before being sacrificed. After the cornea and lens were removed, a piece of retina was flattened on a membrane filter (Merck Milli-

pore, HAWP01300). Then the whole-mounted retina was incubated in Ames' medium and maintained at 31°C to 33°C.³³ TdTomato-expressing cells were identified with a brief snapshot of fluorescence excitation light.³⁴ An intracellular electrophysiological recording was then performed at tdTomato-positive cells. Light spots at different size gradients with a 2-second ON and 8-second OFF repeated three times and generated by a customized projector were casted over the retina through the 40× objective lens. The responses to spots were recorded under the current clamp. The intracellular solution contained: 121 mM potassium gluconate, 4 mM KCl, 10 mM HEPES, 0.2 mM EGTA, 4 mM MgATP, 0.3 mM Na₃GTP, 5 mM sodium phosphocreatine, and 13.4 mM biocytin (pH adjusted to 7.25 with KOH). The light intensity was calibrated to 6.2 log photons/μm²/s.^{24,26} The latency time to peak response is defined by the time from light onset or offset to peak response.

Morphological Reconstruction

After the electrophysiological recording, that piece of retina was transferred to a 24-well plate as soon as possible. Retinas were fixed 2 hours in 4% PFA, and then washed three times with 1× PBS. Retinas were blocked by 3% BSA in PBS for 2 hours at RT. After that, retinas were incubated at 3% BSA solution containing streptavidin, Alexa Fluor 488 (ThermoFisher Scientific, S11223, 1:500) overnight at 4°C. Retinas were washed three times for 10 minutes each and then mounted with anti-fade mounting medium (ThermoFisher Scientific, S36972). The morphology of ACs were captured under 20 × (N.A. 0.8) dry objective with a Zeiss LSM 980 confocal microscope, scanned in Z-stacks at a step of 0.6 μm with laser 488 nm. A snap under 488 nm and 555 nm was captured to ensure the morphologies were representative of tdTomato-positive cells. The captured confocal images were imported to the NeuroLucida software (MFB Bioscience, Williston, VT). The dendrites were manually reconstructed according to the recommendation of NeuroLucida software. Dendritic field size and number of branchpoints were calculated using Python script.³⁵ The maximum diameters were determined as the maximum length of the convex hull of the dendritic trees.

Patch-seq Procedure

TdTomato-positive cells were identified by LED illumination (540–580 nm) and targeted for whole-cell patch recording.³⁶ Transcriptomes of tdTomato-positive cells were collected according to previously published Patch-seq protocols.²⁹ Briefly, all working surfaces and equipment that came into contact with experimenters were cleaned thoroughly using RNaseZAP and 75% (vol/vol) ethanol. Recording pipettes of 5 to 7 MΩ were chosen because ACs were quite small. Internal solution containing 111 mM potassium gluconate, 10 mM HEPES, 0.2 mM EGTA, 4 mM KCl, 4 mM MgATP, 0.3 mM Na₃GTP, 5 mM sodium phosphocreatine, and 13.4 mM biocytin was prepared as described previously.³⁷ Before each experiment, we added 5 μL recombinant RNase inhibitor into 495 μL internal solution. Morphological recovery was not done in this study. It took 5 to 10 minutes for the AC to swell to a proper size. We tended to reposition the pipette frequently to keep it at the side of the cell. After recording, the cell contents were sucked into a patch pipette and ejected into a 0.2-mL RNase-free PCR tube which contains 4 μL of lysis buffer.

Preparation of the Full-length RNA Sequencing (RNA-seq) Library and Sequencing

Single cell RNA was converted to cDNA according to the previous protocol.^{29,38} Briefly, samples were denatured at 72 °C for 3 minutes and a reverse transcription mix was assembled as following (dosage of reagent for one sample was listed as an example): 2 µL Superscript II first-strand buffer (5×), 2 µL Betaine (5 M), 0.5 µL Superscript II Reverse Transcriptase (200 U/µL), 0.5 µL DTT (0.1 M), 0.29 µL nuclease-free sterile water, 0.25 µL recombinant RNase inhibitor (40 U/µL), 0.1 µL LNA-TSO (100 µM), and 0.06 µL MgCl₂ (1 M). The reverse-transcription reaction was run at 42°C for 90 minutes followed by 10 cycles at 50°C for 2 minutes and 42°C for 2 minutes. The enzyme was inactivated by holding at 70°C for 15 minutes. Reagents for amplification of one sample are as follows: 12.5 µL KAPA HiFi HotStart ReadyMix (2×), 2.25 µL nuclease-free sterile water, and 0.25 µL IS PCR primers (10 µM). The PCR program, containing (1) 98°C for 3 minutes; (2) 18 cycles of 98°C for 20 seconds, 67°C for 15 seconds, and 72°C for 6 minutes; (3) 72°C for 5 minutes, was used. Purification was conducted according to previous protocol. Final sequencing libraries were constructed using a Nextera Kit according to manufacturer's instructions (Nextera XT DNA Library Prep Reference Guide, version May 2019; Illumina, San Diego, CA). The constructed cDNA library was sequencing on the Novaseq 6000 System (Illumina). Each cDNA sample was sequenced to 10 million reads.

Sequencing Data Processing

We aligned 150 bp paired-end sequencing reads with the GRCh38 (mm10) mouse reference genome using STAR (version 2.7.0)³⁹ via the function two pass mode. The total gene counts matrix including exonic and intronic reads were calculated and generated using the RSEM (RNA-Seq by expectation maximization) package.⁴⁰ We used Scanpy (version 1.7.1) to analyze and visualize. Cells with gene numbers of less than 2000 and mitochondrial genes more than 5% were filtered. The data were log-normalized and scaled to 10000 transcripts per cell. Patch-seq dataset were visualized using a uniform manifold approximation and projection.

RESULTS

A Subset of TH-negative Cells in the Retina Was Labeled in DAT-tdTomato Mouse

By crossing DAT-Cre (Strain #006660) with Ai9 (Strain #007909), we found that tdTomato-positive cells distributed evenly in the whole-mounted retinas (Fig. 1A). The majority of somata were located at the INL and the others were occasionally displaced in the GCL (Fig. 1B). A complete count of these cells yielded 1070.3 ± 58.5 per retina (mean ± SD; *n* = 3).

We then reconstructed the morphologies of tdTomato-positive cells (Fig. 1C and Supplementary Figs. S1A–B). Fluorescently labeled cells in the INL and GCL had an average maximum diameter of 1.45 ± 0.18 mm (INL; *n* = 4 cells; 4 retinas) and 1.36 ± 0.19 mm (GCL; *n* = 4 cells; 4 retinas), respectively. The average arbor size of tdTomato-positive cells in INL and GCL were 0.80 ± 0.30 mm² (INL; *n* = 4 cells; 4 retinas) and 0.84 ± 0.21 mm² (GCL; *n* = 4 cells; 4 retinas).

The number of branchpoints of cells in INL and GCL were 27 ± 4 (INL; *n* = 4 cells; 4 retinas) and 19 ± 2 (GCL; *n* = 4 cells; 4 retinas) (Supplementary Fig. S1C). In conclusion, cells in the retinas of DAT-tdTomato mouse line were wide-field ACs. And there were no morphological differences between cells in INL and GCL (Supplementary Fig. 1C).

However, we found that no TH-positive cells (0%; *n* = 122 cells; *n* = 13 retinas; *n* = 10 mice) (Table 2) colocalized with tdTomato immunoreactivity in mouse retina, proved by immunostaining in both whole-mounted retinas (Fig. 1D) and vertical retinal sections (Figs. 1E–F). Traditionally, the IPL of retina can be divided into five sublaminae (Supplementary Figs. S1 to S5).^{9,41} While the dendrites of dopaminergic ACs stratified in S1,^{42,43} the dendrites of DAT-tdTomato cells stratified in the border between S2 and S3, forming a distinct line parallel to that of dopaminergic ACs (Figs. 1E–F).

To confirm that the transgenic mouse we used was the traditional DAT-Cre line,⁴⁴ we conducted immunostaining in the brain sections. In accordance with expectation, most dopaminergic neurons in the substantia nigra pars compacta were labeled in this DAT-tdTomato mouse line, proved by the colocalization of TH immunoreactivity with tdTomato expression (Fig. 1G, Supplementary Figs. S2A–C). To sum up, we thought that the Cre recombinase expression pattern in this transgenic mouse showed an ectopic mode in the retina, not in the substantia nigra pars compacta.

DAT-tdTomato-Positive Neurons in Retina Are GABAergic ACs

It was obvious that fluorescently labeled cells in the retinas of DAT-tdTomato mice were ACs according to their distinct morphology. Several authentic AC types have been well-studied in previous studies. The majority of ACs are inhibitory neurons that use GABA or glycine as neurotransmitters, which are GABAergic or glycinergic ACs, respectively.⁴⁵ There is a type of excitatory ACs that uses glutamate as a neurotransmitter that have also been found.^{46,47} In addition, there are some other subpopulations, for instance, non-GABAergic non-glycinergic ACs expressing no GABAergic, glycinergic or glutamatergic markers,⁴⁸ SACs, which are cholinergic ACs,⁴⁹ and the A-II amacrine neurons strongly express the *Gjd2* gene.⁵⁰

To determine which kind of ACs the tdTomato-positive cells belonged to, retinal sections prepared from DAT-tdTomato mice were first immunostained for several inhibitory neuronal biomarkers. Almost all tdTomato-positive cells examined were found to exhibit the immunoreactivity for GABAergic neuron markers glutamic acid decarboxylase (GAD) 67 (INL, 100%, 71 of 71 cells; GCL, 100%, 7 of 7 cells; *n* = 5 retinas; *n* = 5 mice) (Fig. 2A and Table 2), GAD65 (INL, 97.7%, 87 of 89 cells; GCL, 100%, 8 of 8 cells; *n* = 7 retinas; *n* = 7 mice) (Fig. 2B and Table 2), and GABA (INL, 94.1%, 159 of 169 cells; GCL, 100%, 18 of 18 cells; *n* = 15 retinas; *n* = 12 mice) (Fig. 2C and Table 2). None of tdTomato-positive cells (0%, 43 cells; *n* = 6 retinas; *n* = 6 mice) (Fig. 2D and Table 2) colocalized with glycine transporter 1 (GlyT1) immunoreactivity, a marker for glycinergic neurons.

Additional immunostaining experiments further proved that almost none of tdTomato-positive cells colocalized with choline acetyltransferase (ChAT) (0%, 0 of 65 cells; *n* = 4 retinas; *n* = 4 mice) (Fig. 3A and Table 2), vasoactive

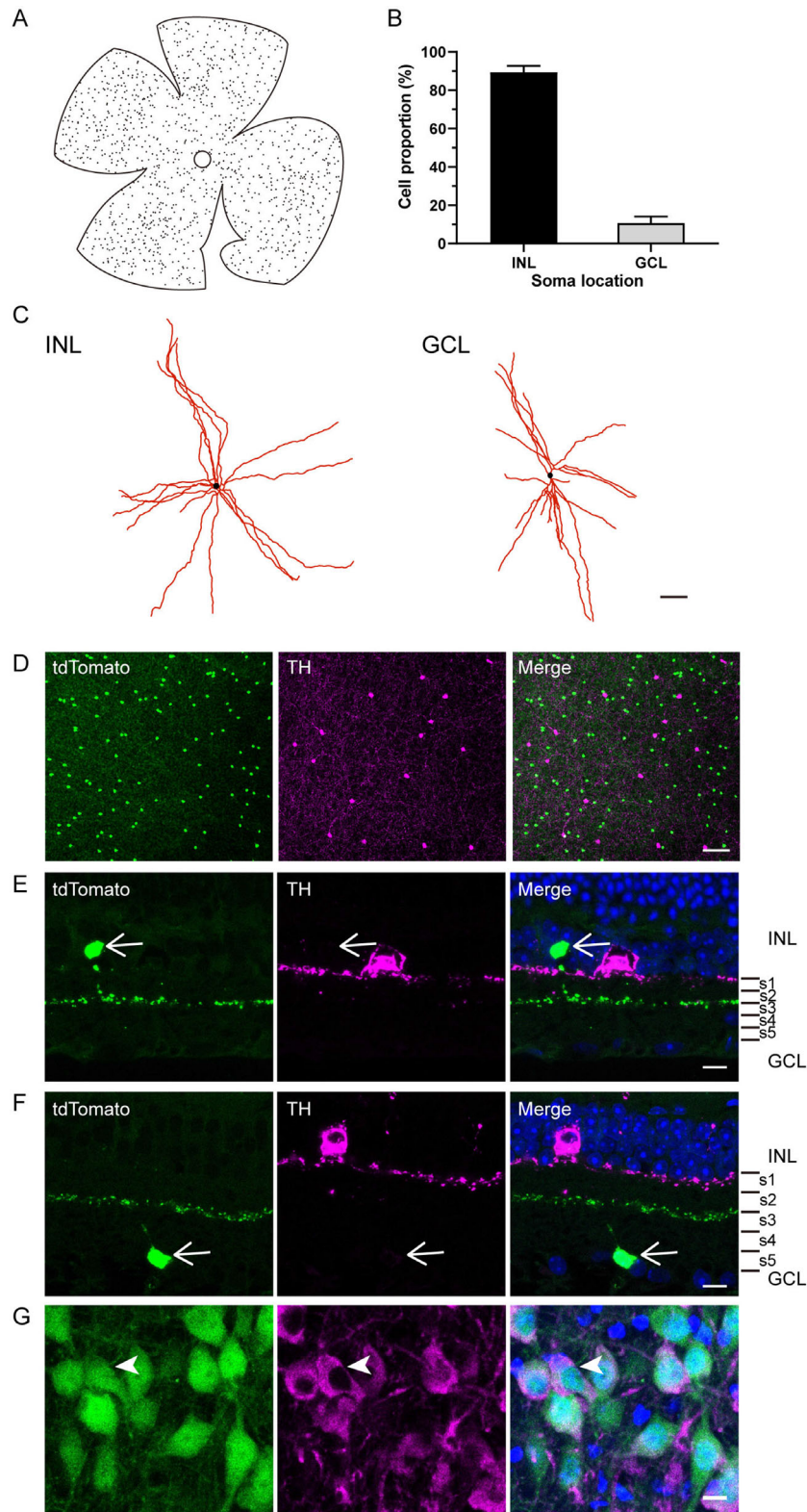


FIGURE 1. DAT-tdTomato mouse labels a subset of TH-negative retinal cells. **(A)** A silhouette showing the distributions of fluorescent cells labeled by DAT-tdTomato mouse. **(B)** Bar chart summarizing the percentages of somata located in INL and GCL. **(C)** Examples demonstrating the morphologies of fluorescent cells located in INL and GCL labeled in the DAT-tdTomato mouse. Scale bar, 200 μ m. **(D)** Representative images captured from whole-mounted retinas prepared from DAT-tdTomato mice stained with TH. Images were taken at the level of INL due to the TH cells located in INL. Scale bar, 100 μ m. **(E)** Vertical retinal sections from DAT-tdTomato retinas were stained with TH. Scale bar, 10 μ m. **(F)** Same as **(E)**, except that a tdTomato-positive cell located in the GCL was chosen as an example. **(G)** Representative images of vertical sections of substantia nigra pars compacta stained with TH. Scale bar, 10 μ m. It is clear that tdTomato-positive cell and TH-positive cells do not colocalize in the retina (*white arrow*) (*right* in **E** and **F**), but colocalize in the substantia nigra pars compacta (*arrowhead*) (*right* in **G**). As shown in the merged images, dendrites of tdTomato-positive cells lie in the border between S2 and S3.

TABLE 2. Statistics for Colocalization of TdTomato-positive Cells With a Number of Molecular Markers

Soma Location	Cell Marker	TdTomato + Cell Counted	Marker-labeled TdTomato + Cells (%)	No. of Retinas	No. of Mice
INL	GABA	169	159 (94.1)	15	12
	GAD67	71	71 (100)	5	5
	GAD65	89	87 (97.7)	7	7
	GlyT1	43	0 (0)	6	6
	vGluT3	56	0 (0)	6	6
	TH	122	0 (0)	13	10
	VIP	48	0 (0)	4	4
	Calretinin	126	89 (70.6)	12	8
	ChAT	65	0 (0)	4	4
	5T4	257	250 (97.3)	20	20
GCL	GABA	18	18 (100)	15	12
	GAD67	7	7 (100)	5	5
	GAD65	8	8 (100)	7	7
	5T4	22	21 (95.5)	18	16
	Calretinin	15	13 (86.7)	12	10

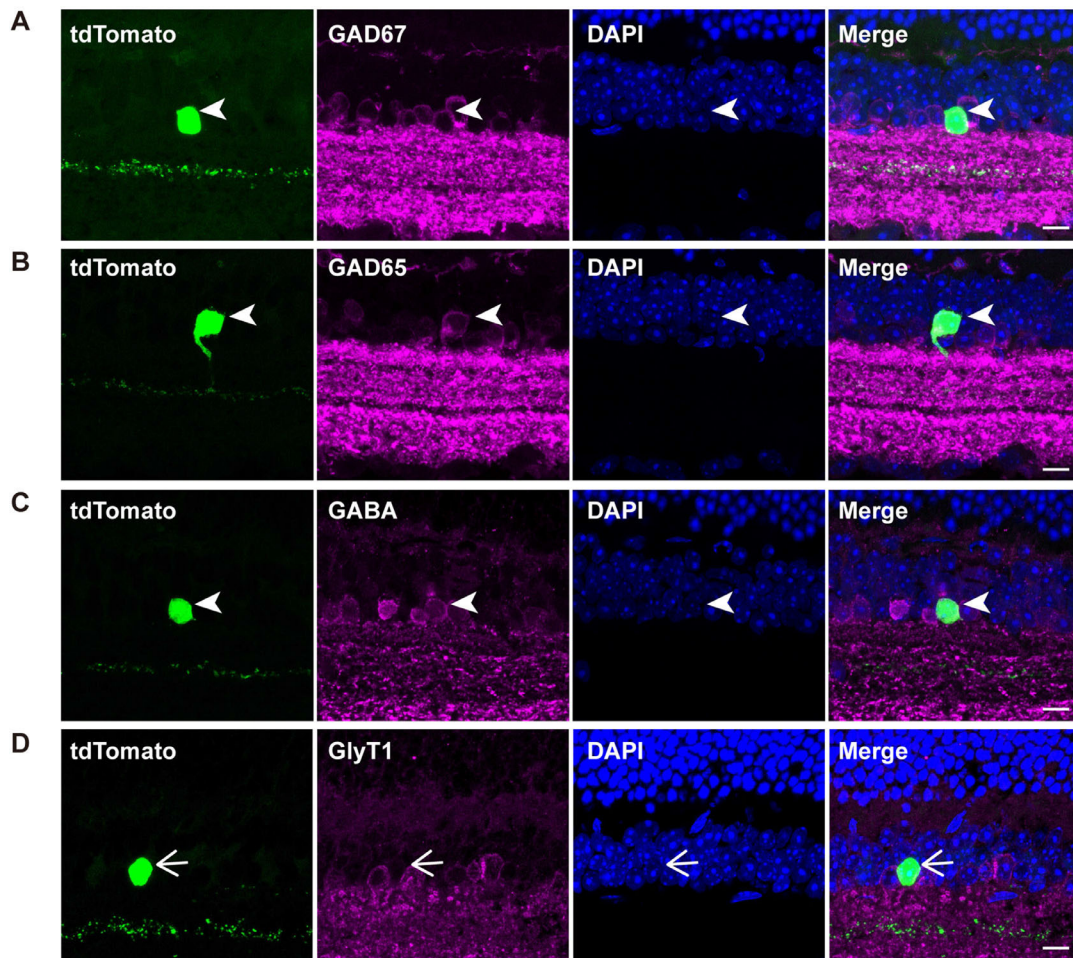


FIGURE 2. TdTomato immunoreactivity in retina of DAT-tdTomato transgenic mouse is localized to GABAergic ACs. Representative immunostaining images of retinal sections stained with known biomarkers for inhibitory ACs, including GAD67 (A), GAD65 (B), GABA (C), and GlyT1 (D). Note the presence of immuno signals for GAD67, GAD65 and GABA (arrowheads) and absence of immuno signals for GlyT1 (arrows) in tdTomato-positive cells. Scale bar, 10 μ m.

intestinal peptide (VIP) (0%, 0 of 48 cells; $n = 4$ retinas; $n = 4$ mice, Fig. 3B and Table 2), vesicular glutamate transporter 3 (VGLUT3) (0%, 0 of 56 cells; $n = 6$ retinas; $n = 6$ mice) (Fig. 3C and Table 2), immunoreactivity, indicating that DAT-tdTomato cells were not SACs,⁴⁹ VIP-expressing ACs,⁵¹ or

VGLUT3-expressing ACs.⁴⁶ It has been reported that there is one AC type (0.3% of all ACs) expressing the gene *VGlut1*.⁴⁷ However, the protein VGlut1 has been proved to be absent in the INL, meaning that VGlut1 is not expressed in the cell bodies of ACs.⁵² For this reason, it seems not necessary

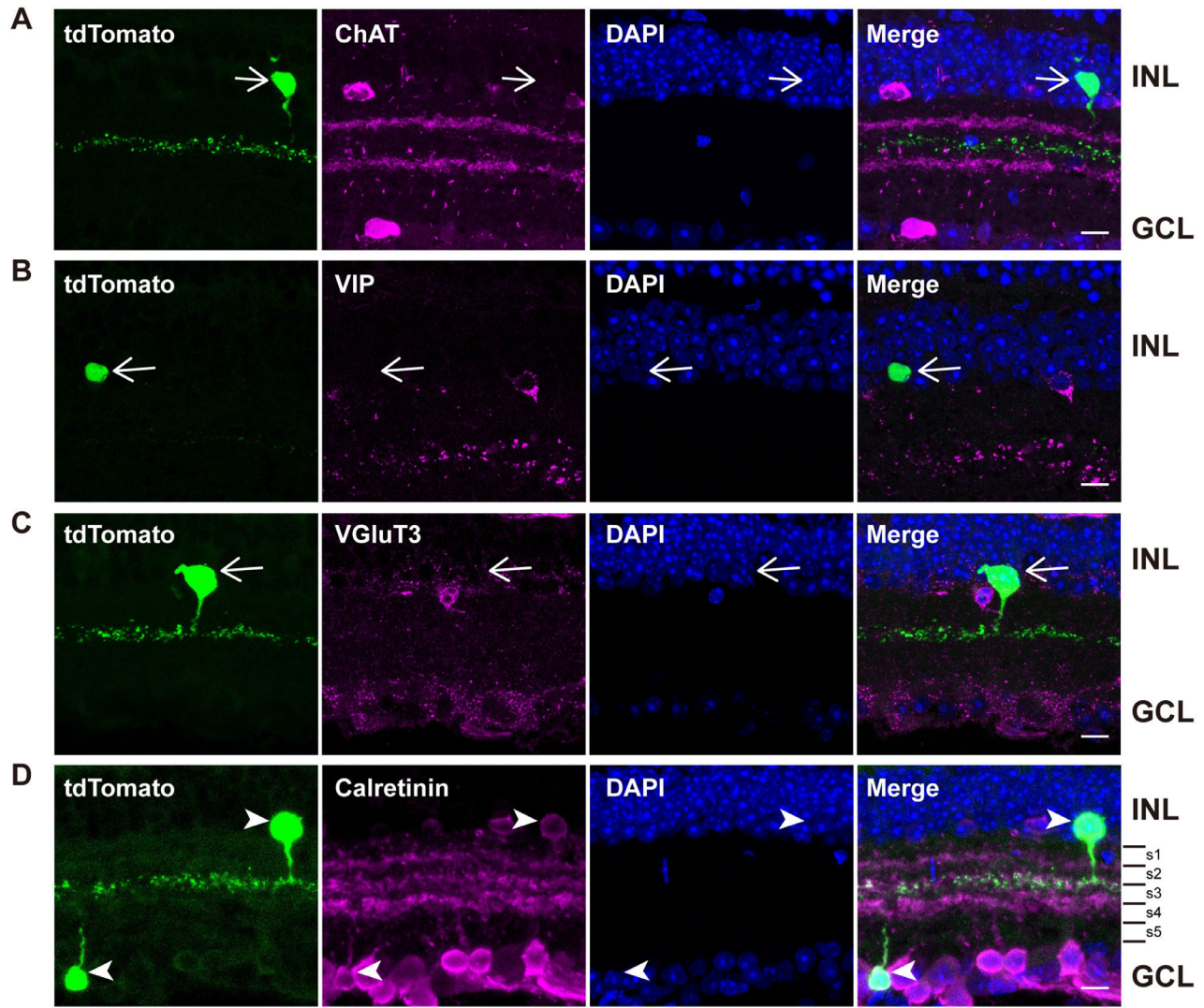


FIGURE 3. Other known AC markers immunoreactivity is absent in tdTomato-positive cells except for calretinin. Representative immunostaining images of DAT-tdTomato retinal sections stained with ChAT (A), VIP (B), VGLUT3 (C), and calretinin (D). What can be seen is that tdTomato-positive cells lack immunoreactivity for ChAT, VIP and VGLUT3 (arrows), but are immunopositive to calretinin (arrowheads). Scale bar, 10 μ m.

to stain tdTomato-positive cells with VGLUT1 antibody. We also found the majority of tdTomato-positive cells were immunoreactive to calretinin (INL, 70.6%, 89 of 126 cells; GCL, 86.7%, 13 of 15 cells; $n = 12$ retinas; $n = 8$ mice) (Table 2) and tdTomato immunoreactivity was coincident with calretinin immunoreactivity in the border of S2 and S3 (Fig. 3D).

Expression Patterns of Known Marker Genes for ACs Are Consistent With Immunostaining Results

Next, we would like to profile DAT-tdTomato cells in the retina using single-cell RNA-seq (scRNA-seq), which might provide us more comprehensive information compared with traditional immunostaining strategies. To this end, Patch-seq was conducted in vertical slices prepared from DAT-tdTomato retinas. Briefly, whole-cell patch clamp recordings were performed in tdTomato-positive cells targeted under 530 to 550 nm fluorescence. The cell contents were aspi-

rated into the pipette and were then used in the subsequent Smart-seq2 procedure (Fig. 4A).²⁹ In total, we collected transcriptomes from 190 tdTomato-positive cells and 152 passed initial quality control. The mRNA of these 152 cells were sequenced, yielding on average 4.04 ± 1.33 million reads (mean \pm SD; on a \log_{10} scale, 15.10 ± 0.76) and 7160 ± 1400 (mean \pm SD) detected genes per cell (Supplementary Figs. S3A–D). Preliminary analysis of these Patch-seq transcriptomes indicated low percent of counts mapping to mitochondrial genes (Supplementary Fig. S3A), a high sequencing depth (Supplementary Fig. S3B), and a normal distribution of cells with different reads (Supplementary Fig. S3C). The relationship between sequencing depth and the number of detected genes per cell was also shown in Supplementary Fig. S3D. These data demonstrated the high quality of our Patch-seq dataset.

Using these high-quality transcriptomes, we first examined the expression patterns of marker genes for main retinal cell types. We found Patch-seq cells showed a high expression of marker genes for ACs (*Pax6* and *Slc32a1*)

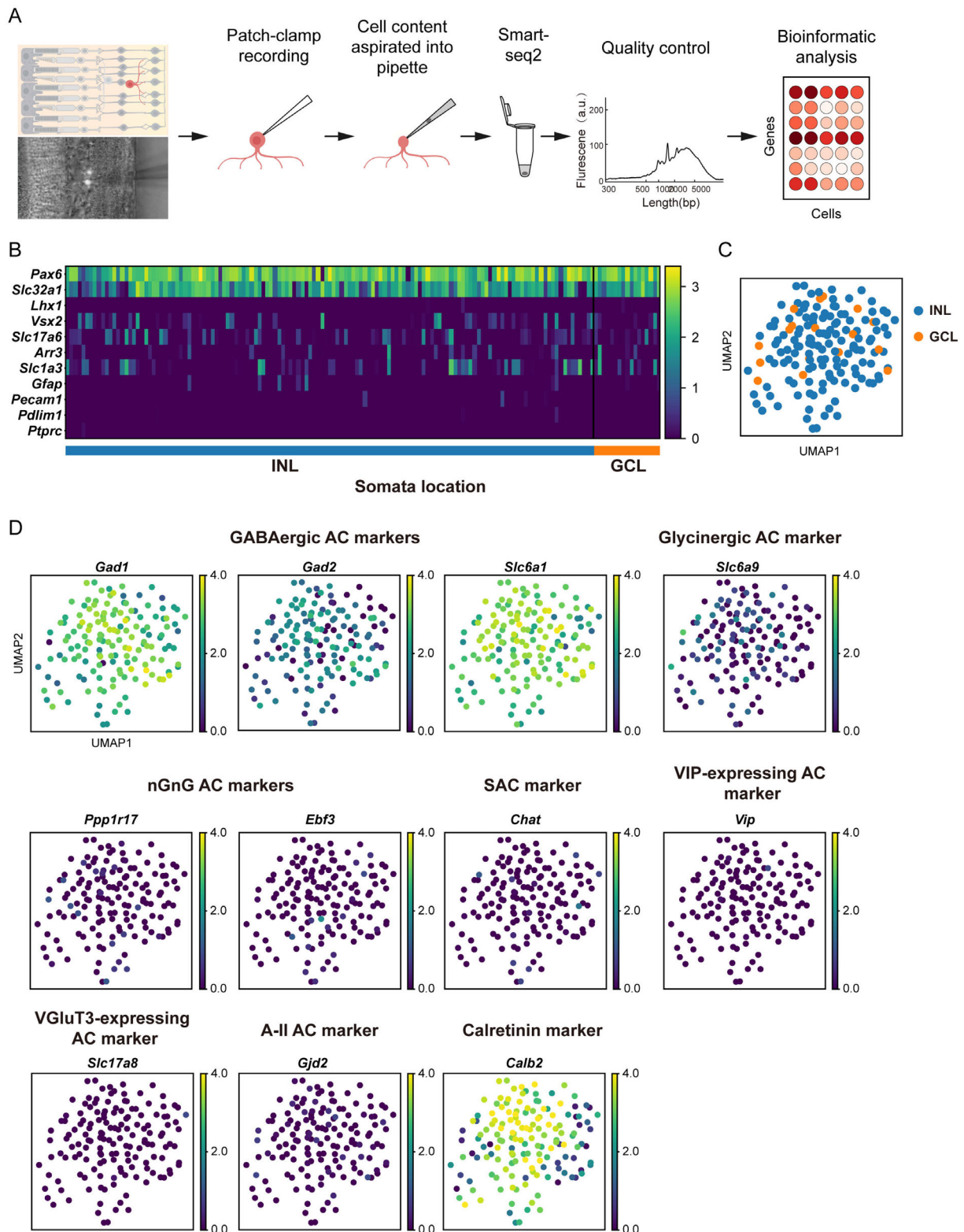


FIGURE 4. Patch-seq of tdTomato-positive cells of retinal sections. **(A)** Schematic of the Patch-seq procedure in this paper (created with [BioRender.com](https://www.biorender.com)). **(B)** Expression patterns of a subset of marker genes for retinal cell classes and types. *Pax6* and *Slc32a1* are marker genes for ACs; *Lhx1* for horizontal cells; *Vsx2* for bipolar cells; *Slc17a6* for RGCs; *Arr3* for cones; *Slc1a3* for Müller cells; *Gfap* for Astrocytes; *Pecam1* for endothelium; *Pdlim1* for pericytes and *Ptprc* for microglia. INL: cell bodies in the INL ($n = 135$ cells); GCL: cell bodies in the GCL ($n = 17$ cells). **(C)** Uniform manifold approximation and projection (UMAP)s showing the distribution of Patch-seq ACs ($n = 152$ cells) with cell bodies located in GCL ($n = 17$ cells) and INL ($n = 135$ cells). **(D)** UMAPs showing the expression of marker genes of known AC types. *Gad1*, *Gad2*, and *Slc6a1* are the marker genes for GABAergic ACs; *Slc6a9* for glycinergic ACs; *Ppp1r17* and *Ebf3* for non-GABAergic non-glycinergic ACs; *Chat* for SACs; *Vip* for VIP-expressing ACs; *Slc17a8* for VGlut3-expressing ACs; *Gjd2* for A-II ACs; and *Calb2* for calretinin. It can be seen that tdTomato-positive cells highly express markers of ACs and GABAergic neurons, as well as gene encoding calretinin.

and a low expression of marker genes for other cell types in retina (*Lhx1* for horizontal cells, *Vsx2* for bipolar cells, *Slc17a6* for RGCs, *Arr3* for cones, *Slc1a3* for Müller cells, *Gfap* for Astrocytes, *Pecam1* for endothelium, *Pdlim1* for pericytes and *Ptprc* for microglia) (Fig. 4B). Therefore, these fluorescently labeled cells were ACs, consistent with their morphological characteristics shown elsewhere in this article.

Because our Patch-seq dataset was harvested from cells located in both the INL ($n = 137$) and the GCL ($n = 15$), we wondered if there is a gene expression difference between them. However, these two types of cells cannot be divided into two clusters in the uniform manifold approximation and projection (Fig. 4C), suggesting the transcriptomic similarities between cells in the INL and GCL. Nevertheless, we provided the differentially expressed genes between these two groups (Supplementary Table S1).

Next we plotted the expression patterns of marker genes for main AC types using uniform manifold approximation and projections, including (1) *Gad1*, *Gad2*, and *Slc6a1* encoding GAD67, GAD65, and GABA transporter 1 for GABAergic ACs; (2) *Slc6a9* encoding GlyT1 for glycinergic ACs; (3) *Ebf3* and *Ppp1r17* encoding early B-cell factor and protein phosphatase 1 regulatory subunit 17 for non-GABAergic non-glycinergic ACs^{53,54}; (4) *Chat* encoding ChAT, which is the marker gene for SACs; (5) *Vip* encoding VIP for VIP-expressing ACs; (6) *Slc17a8* encoding VGLuT3 for VGLuT3-expressing ACs; (7) *Gjd2* encoding connexin-36 for A-II ACs; and (8) *Galb2* encoding calretinin (Fig. 4D). Consistent with the immunostaining results presented elsewhere in this article, Patch-seq cells highly expressed marker genes for GABAergic ACs, *Gad1*, *Gad2*, *Slc6a1*, and calretinin-encoding gene *Galb2*.

TdTomato-Positive Cells in Retina Are TPBG-expressing ACs

Apart from the canonical taxonomy based on morphology or neurotransmitters mentioned elsewhere in this article, recently, mouse retinal ACs have been classified solely according to their transcriptomes, bringing forth 21 or 63 molecularly defined clusters.^{47,53} Thus, we examined if the ACs labeled in DAT-tdTomato mice were part of these molecularly distinct clusters.

Surprisingly, from our observation, it revealed the highly selective expression of *Tpb_g*, a marker gene of cluster 5 (C5) defined by Macosko et al.⁵³ and C25/C31 defined by Yan et al.⁴⁷ (Figs. 5A–B). To demonstrate that these fluorescently labeled cells were certainly belonging to C5 or C25/C31 in these two datasets, we next comprehensively compared our Patch-seq transcriptomes with these datasets, including all 77 cells from C5⁵³ and 913 cells from C25 and C31.⁴⁷ The expression patterns of the known markers of amacrine types (Fig. 5A) and candidate markers of amacrine subpopulations (Fig. 5B), showed a strong consistency within the three datasets.

To confirm our findings, immunostaining experiments were conducted in both vertical retinal sections and whole-mounted retinas. In agreement with transcriptomic characteristics, 5T4 (TPBG) immunoreactivity could be detected in nearly all tdTomato-positive cells (INL, 97.3%, 250 of 257 cells; $n = 20$ retinas; $n = 20$ mice; GCL, 95.5%, 21 of 22 cells) (Figs. 5C–F and Table 2). As shown in Figure 5D, the tdTomato-positive cells located in the GCL were also labeled with an antibody directed to 5T4.

To summarize, our results suggested that cells labeled by DAT-tdTomato mice in the retina were part of molecularly defined clusters, namely, C5 and C25/C31. This finding indicated that a subset of ACs with transcriptomic similarity in the retina were selectively labeled by DAT-tdTomato transgenic mice.

The DAT-tdTomato Cells Show an ON–OFF Response to Light Stimulation

We next carried out patch-clamping on the fluorescent cells in the whole-mounted retinas to identify their light-responsive characteristics (Fig. 6A). All recorded tdTomato-positive cells ($n = 21$) showed an ON–OFF response to light stimulation (depolarized when light both increments and decrements). It was not surprising, considering the exclusive dendritic stratification in the IPL of fluorescently labeled ACs. In an analogous study,⁵⁵ a unique subtype of ACs was identified in rabbit retinas, which stratified within S3 and showed an ON–OFF response to light stimulation. We next used concentric spots of light of increasing size, centering on the focus of the receptive fields of the target cells (Fig. 6B). The ON and OFF responses steadily increased along with the expanding spot (50 μ m, 100 μ m, 150 μ m, 175 μ m, 250 μ m, 350 μ m, and 650 μ m) (Fig. 6C). The time to peak depolarization between ON and OFF responses exhibited less variability (Fig. 6D).

DISCUSSION

The complexity of neurons resides in their diverse molecular, morphological, and functional properties. It is believed that the only realistic way to manage this complexity is to group neurons into types.⁵⁶ There are five main neuronal classes in the retina, including sensory neurons (photoreceptors), interneurons (horizontal cells, bipolar cells, and ACs) and projection neurons (RGCs). Among them, ACs, the inhibitory interneurons in the retina, are known for their highest degree of diversity in both morphology and function.⁵⁷ Numerous studies have been done to identify this diversity and further establish transgenic animal lines to approach one of these subtypes.⁵⁸ In this study, we have revealed the high selectivity of DAT-tdTomato (Ai9) mice. This transgenic line is of great value as a tool to specifically label a subset of TPBG-expressing GABAergic ACs.

Collectively, TH2 ACs are wide field with distinct dendrites band located in the middle of IPL,^{23,24} like the wide-field ACs stratifying in the stratum 3 of the IPL (WA3-2 cells) in a previous study.⁵⁹ TH2 ACs are GABAergic and can be stained with calretinin antibody.²⁴ They also show an ON–OFF response to light stimulation.²⁴ The fluorescent cells in the retina of DAT-tdTomato Ai9 mice share these characteristics with TH2 ACs.

The lack of detectable TH within TH2 cells may result from the higher sensitivity of transgenic reporter than immunocytochemistry.²³ Some also suppose that the low TH level or the existence of TH2 ACs-specific enzyme isoforms may be the reasons.²⁴

In this study, we provide a detailed investigation of a mouse line DAT-Cre crossed with the tdTomato reporter line Ai9, which has more specific expression in TH2 ACs compared with the previously published DAT-Cre lines crossed with a different reporter line (Ai14).¹⁴ A comparison

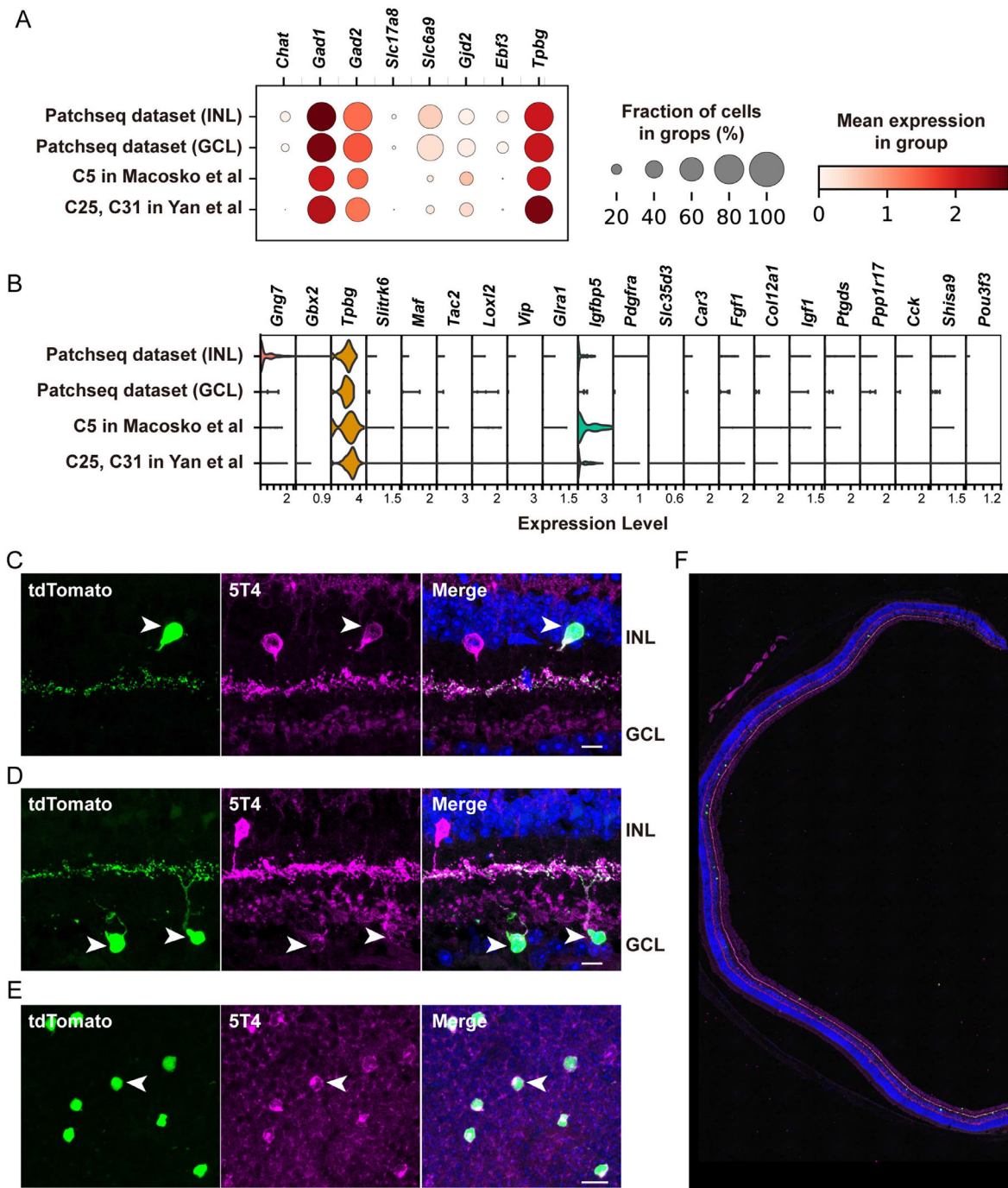


FIGURE 5. TdTomato-positive cells exhibit robust TPBG (5T4) immunoreactivity. **(A)** A comparison of expression patterns of known markers of AC types among our Patch-seq dataset (INL, cell bodies in the INL [$n = 135$ cells]; GCL, cell bodies in the GCL [$n = 17$ cells], C5 in Macosko et al.⁵³ [$n = 77$ cells] and C25/C31 in Yan et al.⁴⁷ [$n = 913$ cells]). **(B)** A comparison of expression patterns of candidate markers of AC subpopulations within these four datasets. **(C)** Vertical retinal sections prepared from DAT-tdTomato retinas were immunolabeled with antibodies probing 5T4. Scale bar, 10 μ m. **(D)** Same as **(C)**, but captured from tdTomato-positive cells located in GCL. Scale bar, 10 μ m. **(E)** Images of whole-mounted retina immunostained with antibody against 5T4. Images were taken in z-stack mode from GCL to INL. Orthogonal Projection method was used to display the images on the x-y plane. Scale bar, 200 μ m. **(F)** An overall view of retinal sections double-labeled with tdTomato and 5T4. Scale bar, 200 μ m. Note that tdTomato-positive cells (arrowheads) located both in the INL and GCL are colocalized with 5T4 immunoreactivity.

among four transgenic mouse lines is exhibited in Supplementary Table S2. Using the Patch-seq technique, we confirmed the transcriptomic, physiological, spatial, and functional properties of the labeled cells. We provide a tran-

scriptomic dataset directly collected from TH2 ACs at the single cell resolution and link transcriptomic information with morphological and electrophysiological properties and precise locations. Indeed, this accurate approach revealed

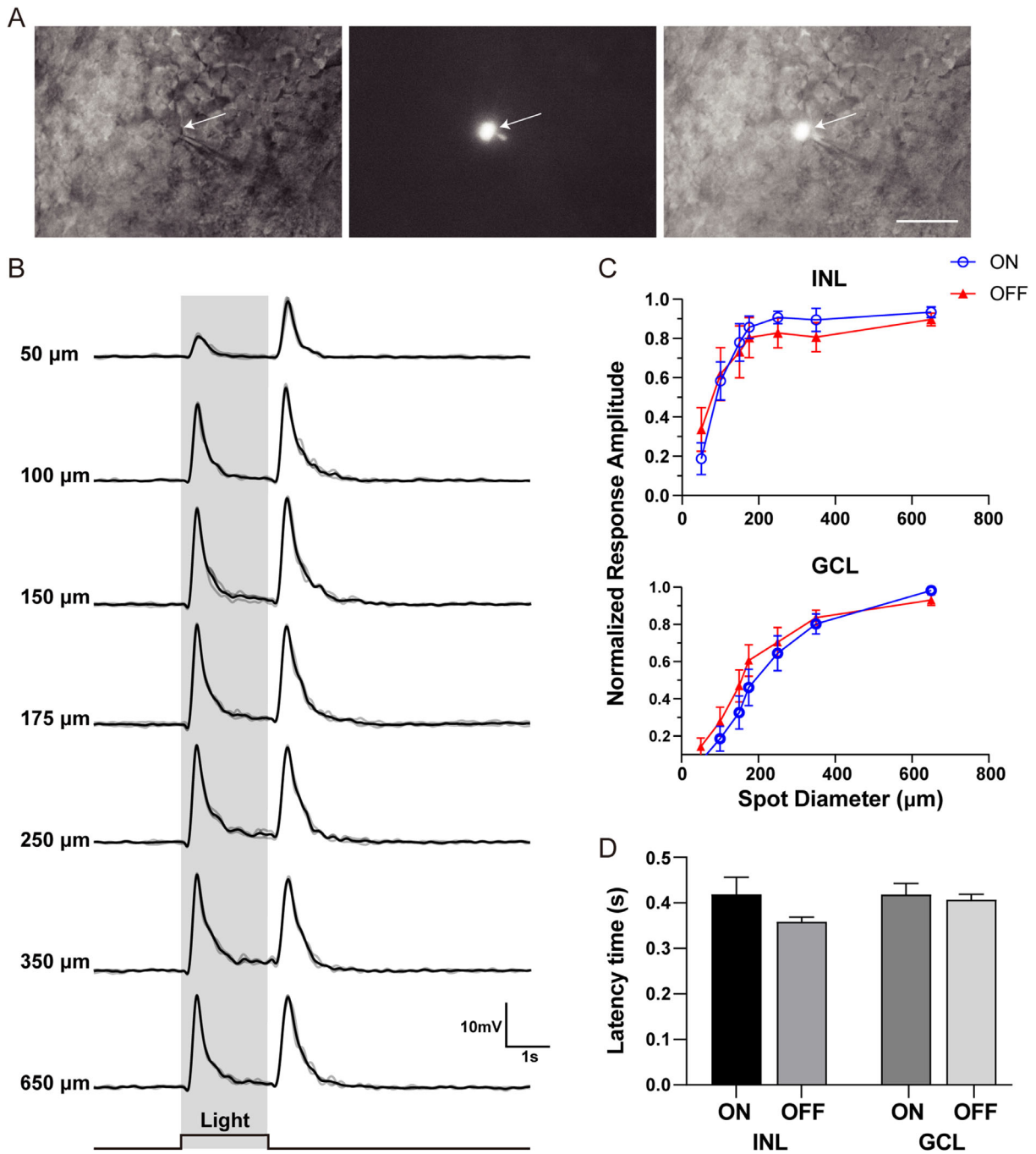


FIGURE 6. Recorded tdTomato-positive cells responded to light stimulation with ON-OFF responses. (A) TdTomato-positive cell (white arrows) under infrared and fluorescent light. Scale bar, 10 μm. (B) Responses of a fluorescent cell located in the GCL to visual stimulation in the form of light spots projected onto the central portion of the receptive field. The diameter of each spot is listed at the left of each trace. (C) Normalized ON and OFF response amplitudes to different sizes of spots ($n = 21$ cells from 6 DAT-tdTomato mice; INL, $n = 9$; GCL, $n = 12$). (D) Quantification of the latency of the peak light-induced current shows no significant difference between ON and OFF responses (one-way ANOVA with post hoc Tukey's tests, error bars: SEM). The latency time to peak response is defined by the time from light onset or offset to peak response.

novel properties for the TH2 cells. We also identified a new genetic marker *Tpbg*, which is involved in retinal development after birth.⁶⁰ The identification of *Tpbg* provides a powerful genetic handle for further study of the TH2 cells. We believe our study contains sufficient novel discoveries that can contribute to the field in the study of the function of ACs.

TPBG, also known as 5T4, is a type I membrane glycoprotein. In the mouse retina, TPBG is mainly expressed in rod bipolar cells and an uncharacterized group of ACs.⁶⁰ According to studies about the relationship between TPBG and retina, TPBG expression is undetectable in the retina at birth until significant increase before eye opening. The expression of TPBG remained stable until postnatal 11 day

and increased by approximately 10-fold by postnatal day 12.³⁰ It was suggested that TPBG played a potential role in visual system development before and after receiving light stimulus.^{30,60} TPBG has also been reported to selectively label inner midgrid RGCs in the primate retina, suggesting the importance of this protein.^{61,62} The expression pattern of *Tpbg* in ACs of mouse retina has been studied previously in two high-throughput scRNA-seq studies. This gene is identified as a candidate marker of amacrine subpopulations, namely, C5 and C25/C31.^{47,53} But surprisingly, the fact that tdTomato-positive cells in the retinas of DAT-Cre transgenic mice selectively expressed *Tpbg* had not been reported. Although Cre recombinase activity was absent in TH-immunoreactive ACs, it could be present in any other type of neuron. This finding suggested that tdTomato-positive cells labeled by our transgenic mouse might consist of one molecularly defined AC cluster.

Overall, scRNA-seq has been a powerful tool for comprehensive identification and molecular characterization of cell types since developed.^{63,64} In this study, we find it is quite faithful to identify fluorescent cells in transgenic mice based on their transcriptomes. Compared with other scRNA-seq methods, Patch-seq is designed to collect multimodal datasets from single cells.^{1,29,37,65} In coronal brain cortex slices, the morphological recovery of cells after Patch-seq is relatively convenient because the plane of dendrites is parallel to the slice direction. In retinal vertical sections, ACs and RGCs may lose the majority of their dendrites as the planes of their dendrites are vertical to slice direction. In contrast, in the whole-mounted retinas of DAT-tdTomato mice, most fluorescent cells are located at the INL and the recording pipette must pass long distances through the GCL and IPL to reach the somata. The risk of RNase contamination would have been high if we had performed Patch-seq in a deeper layer of the whole-mounted retinas. For those reasons, the preservation of cellular morphology after Patch-seq was not desired in this study. So in this article, we used Patch-seq to collect only transcriptomes from tdTomato-positive cells.

We used the same DAT-Cre (#006660) as Vuong's article.¹⁴ The difference is that we used a different reporter line (Ai9) to cross with the DAT-Cre line. In summary, the DAT-tdTomato mouse line used by Vuong are generated by crossing DAT-Cre (#006660) to a tdTomato reporter line Ai14 (#007914). The DAT-tdTomato mouse line used by us are generated by crossing DAT-Cre (#006660) to Ai9 (#007909). However, completely different groups of ACs have been labeled by that DAT-tdTomato Ai14, for example, their processes were localized in a narrow band in the OFF sublamina and broadly in the ON sublamina of the IPL. Similar phenomenon has also been mentioned in a previous study,⁸ where the expression patterns of tdTomato in several brain areas, such as central amygdala and Purkinje of cerebellum, are also different between transgenic mouse line tdTom^{DAT-Cre} (Ai9) and tdTom^{DAT-Cre} (Ai14).

Acknowledgments

Supported by research grants from Natural Science Foundation of China (81870682, 81961128021, 81721003); the National Key R&D Program of China (2018YFA0108300); the Guangdong Provincial Key R&D Programs (2018B030335001); Local Innovative and Research Teams Project of Guangdong Pearl River Talents Programme (2017BT01S138); CAMS Innovation Fund for Medical Sciences (2019-I2M-5-005); Science and Technology Program of Guangzhou (202007030011, 202007030010,

202007030001); Clinical Innovation Research Program of Guangzhou Regenerative Medicine and Health Guangdong Laboratory (2018GZR0201001); and the China Postdoctoral Science Foundation (2019M663256).

Disclosure: **W. Huang**, None; **Q. Xu**, None; **F. Liu**, None; **J. Su**, None; **D. Xiao**, None; **L. Tang**, None; **Z.-Z. Hao**, None; **R. Liu**, None; **K. Xiang**, None; **Y. Bi**, None; **Z. Miao**, None; **X. Liu**, None; **Y. Liu**, None; **S. Liu**, None

References

- Gouwens NW, Sorensen SA, Baftizadeh F, et al. Integrated morphoelectric and transcriptomic classification of cortical GABAergic cells. *Cell*. 2020;183(4):935–953.e19.
- Kim CK, Adhikari A, Deisseroth K. Integration of optogenetics with complementary methodologies in systems neuroscience. *Nat Rev Neurosci*. 2017;18(4):222–235.
- Daigle TL, Madisen L, Hage TA, et al. A suite of transgenic driver and reporter mouse lines with enhanced brain cell type targeting and functionality. *Cell*. 2018;174(2):45–480.e22, doi:10.1101/224881.
- Peng H, Xie P, Liu L, et al. Morphological diversity of single neurons in molecularly defined cell types. *Nature*. 2021;598(7879):174–181.
- Choi SH, Bylykbashi E, Chatila ZK, et al. Combined adult neurogenesis and BDNF mimic exercise effects on cognition in an Alzheimer's mouse model. *Science*. 2018;361(6406):eaan8821, doi:10.1126/science.aan8821.
- Roy DS, Arons A, Mitchell TI, Pignatelli M, Ryan TJ, Tonegawa S. Memory retrieval by activating engram cells in mouse models of early Alzheimer's disease. *Nature*. 2016;531(7595):508–512, doi:10.1038/nature17172.
- Feng G, Mellor RH, Bernstein M, et al. Imaging neuronal subsets in transgenic mice expressing multiple spectral variants of GFP. *Neuron*. 2000;28(1):41–51.
- Papathanou M, Dumas S, Pettersson H, Olson L, Wallén-Mackenzie Å. Off-target effects in transgenic mice: characterization of dopamine transporter (DAT)-Cre transgenic mouse lines exposes multiple non-dopaminergic neuronal clusters available for selective targeting within limbic neurocircuitry. *eNeuro*. 2019;6(5):ENEURO.198–19.2019, doi:10.1523/ENEURO.0198-19.2019.
- Kim IJ, Zhang Y, Meister M, Sanes JR. Lamina restriction of retinal ganglion cell dendrites and axons: subtype-specific developmental patterns revealed with transgenic markers. *J Neurosci*. 2010;30(4):1452–1462.
- Zhang Y, Kim IJ, Sanes JR, Meister M. The most numerous ganglion cell type of the mouse retina is a selective feature detector. *Proc Natl Acad Sci USA*. 2012;109(36):E2391–E2398.
- Tran NM, Shekhar K, Whitney IE, et al. Single-cell profiles of retinal ganglion cells differing in resilience to injury reveal neuroprotective genes. *Neuron*. 2019;104(6):1039–1055.e12.
- Cui LJ, Chen WH, Liu AL, et al. nGnG amacrine cells and Brn3b-negative M1 ipRGCs are specifically labeled in the ChAT-ChR2-EYFP mouse. *Invest Ophthalmol Vis Sci*. 2020;61(2):14.
- Zhuang X, Masson J, Gingrich JA, Rayport S, Hen R. Targeted gene expression in dopamine and serotonin neurons of the mouse brain. *J Neurosci Methods*. 2005;143(1):27–32.
- Vuong HE, Pérez de Sevilla Müller L, Hardi CN, McMahon DG, Brecha NC. Heterogeneous transgene expression in the retinas of the TH-RFP, TH-Cre, TH-BAC-Cre and DAT-Cre mouse lines. *Neuroscience*. 2015;307:319–337.
- Madisen L, Zwingman TA, Sunkin SM, et al. A robust and high-throughput Cre reporting and characterization system for the whole mouse brain. *Nature Neuroscience*. 2010;13(1):133–140, doi:10.1038/nn.2467.

16. Abraira VE, Kuehn ED, Chirila AM, et al. The cellular and synaptic architecture of the mechanosensory dorsal horn. *Cell*. 2017;168(1-2):295–310.e19.
17. Mariani AP, Hokoc JN. Two types of tyrosine hydroxylase-immunoreactive amacrine cell in the rhesus monkey retina. *J Comp Neurol*. 1988;276(1):81–91.
18. Oh SJ, Kim IB, Lee EJ, Kim KY, Kim HI, Chun MH. Immunocytochemical localization of dopamine in the guinea pig retina. *Cell Tissue Res*. 1999;298(3):561–565.
19. Versaux-Botteri C, Martin-Martinelli E, Nguyen-Legros J, Geffard M, Vigny A, Denoroy L. Regional specialization of the rat retina: catecholamine-containing amacrine cell characterization and distribution. *J Comp Neurol*. 1986;243(3):422–433.
20. Hirasawa H, Betensky RA, Raviola E. Corelease of dopamine and GABA by a retinal dopaminergic neuron. *J Neurosci*. 2012;32(38):13281–13291.
21. Hirasawa H, Contini M, Raviola E. Extrasynaptic release of GABA and dopamine by retinal dopaminergic neurons. *Philos Trans R Soc Lond B Biol Sci*. 2015;370(1672):20140186, doi:10.1098/rstb.2014.0186.
22. Contini M, Lin B, Kobayashi K, Okano H, Masland RH, Raviola E. Synaptic input of ON-bipolar cells onto the dopaminergic neurons of the mouse retina. *J Comp Neurol*. 2010;518(11):2035–2050.
23. Zhang DQ, Stone JF, Zhou T, Ohta H, McMahon DG. Characterization of genetically labeled catecholamine neurons in the mouse retina. *Neuroreport*. 2004;15(11):1761–1765.
24. Knop GC, Feigenspan A, Weiler R, Dedek K. Inputs underlying the ON-OFF light responses of type 2 wide-field amacrine cells in TH::GFP mice. *J Neurosci*. 2011;31(13):4780–4791.
25. Brügger B, Meyer A, Boven F, Weiler R, Dedek K. Type 2 wide-field amacrine cells in TH::GFP mice show a homogeneous synapse distribution and contact small ganglion cells. *Eur J Neurosci*. 2015;41(6):734–747.
26. Kim T, Kerschensteiner D. Inhibitory control of feature selectivity in an object motion sensitive circuit of the retina. *Cell Reports*. 2017;19(7):1343–1350, doi:10.1016/j.celrep.2017.04.060.
27. Liang CQ, Zhang G, Zhang L, et al. Calmodulin bidirectionally regulates evoked and spontaneous neurotransmitter release at retinal ribbon synapses. *eNeuro*. 2021;8(1):ENEURO.0247–20.2020, doi:10.1523/ENEURO.0257-20.2020.
28. Simmons AB, Camerino MJ, Clemons MR, et al. Increased density and age-related sharing of synapses at the cone to OFF bipolar cell synapse in the mouse retina. *J Comp Neurol*. 2020;528(7):1140–1156, doi:10.1002/cne.24810.
29. Cadwell CR, Scala F, Li S, et al. Multimodal profiling of single-cell morphology, electrophysiology, and gene expression using Patch-seq. *Nat Protoc*. 2017;12(12):2531–2553.
30. Wakeham CM, Ren G, Morgans CW. Expression and distribution of trophoblast glycoprotein in the mouse retina. *J Comp Neurol*. 2020;528(10):1660–1671.
31. Munteanu T, Noronha KJ, Leung AC, Pan S, Lucas JA, Schmidt TM. Light-dependent pathways for dopaminergic amacrine cell development and function. *Elife*. 2018;7:e39866, doi:10.7554/eLife.39866.
32. Lammel S, Steinberg EE, Földy C, et al. Diversity of transgenic mouse models for selective targeting of midbrain dopamine neurons. *Neuron*. 2015;85(2):429–438.
33. Ullmann JFP, Moore BA, Temple SE, Fernández-Juricic E, SP Collin. The retinal wholemount technique: a window to understanding the brain and behaviour. *Brain Behav Evol*. 2012;79(1):26–44.
34. Zhang DQ, Zhou TR, McMahon DG. Functional heterogeneity of retinal dopaminergic neurons underlying their multiple roles in vision. *J Neurosci*. 2007;27(3):692–699.
35. Ran Y, Huang Z, Baden T, et al. Type-specific dendritic integration in mouse retinal ganglion cells. *Nat Commun*. 2020;11(1):2101.
36. Stabio ME, Sabbah S, Quattrochi LE, et al. The M5 cell: a color-opponent intrinsically photosensitive retinal ganglion cell. *Neuron*. 2018;97(1):251.
37. Scala F, Kobak D, Bernabucci M, et al. Phenotypic variation of transcriptomic cell types in mouse motor cortex. *Nature*. 2021;598(7879):144–150.
38. Cadwell CR, Scala F, Fahey PG, et al. Cell type composition and circuit organization of clonally related excitatory neurons in the juvenile mouse neocortex. *Elife*. 2020;9:e52951, doi:10.7554/eLife.52951.
39. Dobin A, Davis CA, Schlesinger F, et al. STAR: ultrafast universal RNA-seq aligner. *Bioinformatics*. 2013;29(1):15–21.
40. Li B, Dewey CN. RSEM: accurate transcript quantification from RNA-seq data with or without a reference genome. *Bioinformatics*. 2015;12:323.
41. Wässle H. Parallel processing in the mammalian retina. *Nat Rev Neurosci*. 2004;5(10):747–757, doi:10.1038/nrn1497.
42. Dumitrescu ON, Pucci FG, Wong KY, Berson DM. Ectopic retinal ON bipolar cell synapses in the OFF inner plexiform layer: contacts with dopaminergic amacrine cells and melanopsin ganglion cells. *J Comp Neurol*. 2009;517(2):226–244.
43. Debertin G, Kántor O, Kovács-Öller T, et al. Tyrosine hydroxylase positive perisomatic rings are formed around various amacrine cell types in the mammalian retina. *J Neurochem*. 2015;134(3):416–428.
44. Bäckman CM, Malik N, Zhang Y, et al. Characterization of a mouse strain expressing Cre recombinase from the 3' untranslated region of the dopamine transporter locus. *genesis*. 2006;44(8):383–390, doi:10.1002/dvg.20228.
45. Marc RE, Liu WLS. Fundamental GABAergic amacrine cell circuitries in the retina: Nested feedback, concatenated inhibition, and axosomatic synapses. *J Comp Neurol*. 2000;425(4):560–582, doi:10.1002/1096-9861(20001002)425:4<560::aid-cne7>3.0.co;2-d.
46. Haverkamp S, Wässle H. Characterization of an amacrine cell type of the mammalian retina immunoreactive for vesicular glutamate transporter 3. *J Comp Neurol*. 2004;468(2):251–263.
47. Yan W, Laboulaye MA, Tran NM, Whitney IE, Benhar I, Sanes JR. Mouse retinal cell atlas: molecular identification of over sixty amacrine cell types. *J Neurosci*. 2020;40(27):5177–5195.
48. Kay JN, Voinescu PE, Chu MW, Sanes JR. Neurod6 expression defines new retinal amacrine cell subtypes and regulates their fate. *Nat Neurosci*. 2011;14(8):965–972.
49. Masland RH. The many roles of starburst amacrine cells. *Trends Neurosci*. 2005;28(8):395–396.
50. Feigenspan A, Teubner B, Willecke K, Weiler R. Expression of neuronal connexin36 in AII amacrine cells of the mammalian retina. *J Neurosci*. 2001;21(1):230–239.
51. Akrouh A, Kerschensteiner D. Morphology and function of three VIP-expressing amacrine cell types in the mouse retina. *J Neurophysiol*. 2015;114(4):2431–2438.
52. Johnson J, Tian N, Caywood MS, Reimer RJ, Edwards RH, Copenhagen DR. Vesicular neurotransmitter transporter expression in developing postnatal rodent retina: GABA and glycine precede glutamate. *J Neurosci*. 2003;23(2):518–529, doi:10.1523/jneurosci.23-02-00518.2003.
53. Macosko EZ, Basu A, Satija R, et al. Highly parallel genome-wide expression profiling of individual cells using nanoliter droplets. *Cell*. 2015;161(5):1202–1214.
54. Shekhar K, Lapan SW, Whitney IE, et al. Comprehensive classification of retinal bipolar neurons by single-cell transcriptomics. *Cell*. 2016;166(5):1308–1323.e30.

55. Bloomfield SA, Völgyi B. Response properties of a unique subtype of wide-field amacrine cell in the rabbit retina. *Vis Neurosci.* 2007;24(4):459–469.
56. Zeng H, Sanes JR. Neuronal cell-type classification: challenges, opportunities and the path forward. *Nat Rev Neurosci.* 2017;18(9):530–546.
57. Balasubramanian R, Gan L. Development of retinal amacrine cells and their dendritic stratification. *Curr Ophthalmol Rep.* 2014;2(3):100–106.
58. Martersteck EM, Hirokawa KE, Everts M, et al. Diverse central projection patterns of retinal ganglion cells. *Cell Rep.* 2017;18(8):2058–2072, doi:10.1016/j.celrep.2017.01.075.
59. Lin B, Masland RH. Populations of wide-field amacrine cells in the mouse retina. *J Comp Neurol.* 2006;499(5):797–809.
60. Tsuboi A. LRR-containing oncofetal trophoblast glycoprotein 5T4 shapes neural circuits in olfactory and visual systems. *Front Mol Neurosci.* 2020;13:581018.
61. Peng YR, Shekhar K, Yan W, et al. Molecular classification and comparative taxonomics of foveal and peripheral cells in primate retina. *Cell.* 2019;176(5):1222–1237.e22.
62. Grünert U, Martin PR. Morphology, molecular characterization, and connections of ganglion cells in primate retina. *Annu Rev Vis Sci.* 2021;7:73–103.
63. Zeisel A, Muñoz-Manchado AB, Codeluppi S, et al. Brain structure. Cell types in the mouse cortex and hippocampus revealed by single-cell RNA-seq. *Science.* 2015;347(6226):1138–1142.
64. Gokce O, Stanley GM, Treutlein B, et al. Cellular taxonomy of the mouse striatum as revealed by single-cell RNA-seq. *Cell Rep.* 2016;16(4):1126–1137, doi:10.1016/j.celrep.2016.06.059.
65. Lipovsek M, Bardy C, Cadwell CR, Hadley K, Kobak D, Tripathy SJ. Patch-seq: past, present, and future. *J Neurosci.* 2021;41(5):937–946.